Journal of Power Sources 192 (2009) 165–169

Contents lists available at ScienceDirect

Journal of Power Sources

journal homepage: www.elsevier.com/locate/jpowsour

Short communication

Comparative study of oxygen reduction reaction on $Ru_xM_ySe_z$ (M = Cr, Mo, W) electrocatalysts for polymer exchange membrane fuel cell

K. Suárez-Alcántara [a], O. Solorza-Feria [b,*]

[a] Depto. Ciencia de Materiales, ESFM-IPN, UP-ALM, Zacatenco, G.A. Madero, C.P. 07738, México, D.F., Mexico
[b] Depto. Química, Centro de Investigación y de Estudios Avanzados del IPN, A. Postal 14-740, 07360 México, D.F., Mexico

ARTICLE INFO

Article history:
Received 20 September 2008
Received in revised form 29 October 2008
Accepted 31 October 2008
Available online 7 November 2008

Keywords:
Oxygen reduction reaction
Electrocatalyst synthesis
Ru-based catalyst
Membrane-electrode assembly
PEMFC

ABSTRACT

Electrochemical evaluation of the $Ru_xM_ySe_z$ (M = Cr, Mo, W) type electrocatalysts towards the oxygen reduction reaction (ORR) is presented. The electrocatalysts were synthesized by reacting the corresponding transition metal carbonyl compounds and elemental selenium in 1,6-hexanediol under refluxing conditions for 3 h. The powder electrocatalysts were characterized by scanning electron microscopy (SEM), and X-ray diffraction (XRD). Results indicate the formation of agglomerates of crystalline particles with nanometric size embedded in an amorphous phase. The particle size decreased according to the following trend: $Ru_xCr_ySe_z > Ru_xW_ySe_z > Ru_xMo_ySe_z$. Electrochemical studies were performed by rotating disk electrode (RDE) and rotating ring-disk electrode (RRDE) techniques. Kinetic parameters exhibited Tafel slopes of 120 mV dec^{-1}; exchange current density of around 1×10^{-5} mA cm^{-2} and apparent activation energies between 40 and 55 kJ mol^{-1}. A four-electron reduction was found in all three cases. The catalytic activity towards the ORR decreases according to the following trend: $Ru_xMo_ySe_z > Ru_xW_ySe_z > Ru_xCr_ySe_z$. However this trend was not maintained when the materials were tested as cathode electrodes in a single polymer exchange membrane fuel cell, PEMFC. The $Ru_xW_ySe_z$ electrocatalyst showed poor activity compared to $Ru_xMo_ySe_z$ and $Ru_xCr_ySe_z$ which were considered suitable candidates to be used as cathode in PEMFCs.

1. Introduction

Worldwide interest in clean energy generation systems such as fuel cells technology has motivated research on the synthesis, characterization and evaluation of novel and stable oxygen reduction electrocatalysts for the direct four-electron transfer process to water formation [1–3]. The oxygen reduction reaction (ORR) in acid media has been investigated extensively due to its importance in many energy device applications [4]. The commercial application of this technology relies on the development of an effective electrocatalyst to overcome the inherent slow kinetics and high electrode overpotentials of current ORR electrocatalysts. Several approaches have been explored but essentially the best results are obtained with the use of platinum, platinum-based or noble metal-based nanostructured materials [5,6]. This kind of materials presents adequate activity towards ORR but in addition, the suitable materials should be able to show appropriate long-term stability. Another important factor to be considered in the design of ORR electrocatalysts is the specific application and market. In this field we have reported that Ru-based electrocatalysts in the nanometric size range exhibited attractive kinetic properties as cathode electrodes for polymer exchange membrane fuel cells, PEMFC [7,8]. The present research reported herein is aimed to synthesize, characterize and evaluate Ru-based electrocatalysts for their potential application in PEMFC. Specifically, this paper compares the kinetic performance of bimetallic chalcogenides of the type $Ru_xM_ySe_z$ (M = Cr, Mo W) as ORR cathode electrocatalyst for PEMFC. If successful, these materials can be an alternative to the Pt-cathode electrocatalyst and with potential applications in non-extensive power-demanding fuel cells. The amount of the noble metal (Ru) can be reduced and the activity towards the ORR improved, compared to a pure noble metal electrocatalyst.

Extensive studies has been reported showing that Ru-based materials present catalytic activity towards ORR, but with the incorporation of Se as a second transition metal the activity and selectivity improves significantly [9,10]. The second transition metal was selected by their capability to form compounds having several oxidation states. In this context, the aim of the present study is to compare in terms of ORR kinetics and fuel cell performance, the incorporation of a second metal, within the ruthenium–selenium matrix and to show how a synergistic effect can improve the stability and enhance the catalytic activity of bimetallic chalcogenides.

* Corresponding author. Tel.: +52 55 5747 3715; fax: +52 55 5747 3389.
E-mail address: osolorza@cinvestav.mx (O. Solorza-Feria).

0378-7753/$ – see front matter © 2008 Elsevier B.V. All rights reserved.
doi:10.1016/j.jpowsour.2008.10.118

2. Experimental

2.1. Catalyst synthesis

$Ru_xM_ySe_z$ (M = Cr, Mo or W) electrocatalysts were synthesized by decarbonylation of transition metal carbonyl compounds and selenium as reported elsewhere [6,7]. Briefly, $Ru_3(CO)_{12}$ (Aldrich), $Cr(CO)_6$ (Strem), $Mo(CO)_6$ (Strem) or $W(CO)_6$ (Strem), respectively, and selenium (Strem) reacted in 150 mL of 1,6-hexanediol for 3 h at 230 °C. The un-reacted precursors and the organic reaction medium were eliminated by several washes using organic solvents, and dried overnight at room temperature. The reaction time and experimental conditions were enough to completely decarbonylate the chemical precursors. This synthesis route produced a mixture of clusters of high and low nuclearity.

2.2. Physical characterization

The surface morphology of the particles was examined by scanning electron microscopy (SEM, FEI Sirion XL30) working at 5 kV. Elemental analysis was performed by energy dispersive X-ray spectroscopy (EDS) coupled with the SEM microscope working at 30 kV. Powder X-ray diffraction (XRD) was carried out in a Diffrac Bruker AXS, D8 Advanced Plus Diffractometer operated at 30 mA and 35 kV using a monochromatic Cu Kα radiation (1.54056 Å). A scanning range from 10° to 100° was explored at a scan rate of 0.02° min^{-1}. XRD data were analyzed with the Diffrac Plus and Topas software and the XRD patterns were identified using the JCPDS database.

2.3. Electrochemical set-up and electrode preparation

Detailed descriptions for the rotating disk electrode (RDE) and rotating ring-disk electrode (RRDE) electrochemical set-ups have been described previously [6,7]. RDE measurements were conducted on a thin film catalysts deposited on a glassy-carbon disk electrode (0.07 cm^2) mounted in an interchangeable RDE holder (Pine Instruments). The thin film consisted of 0.1 mg of electrocatalyst deposited on the glassy carbon by means of an electrocatalyst solution according to a method reported previously. The working RRDE used was a disk of glassy carbon covered with 0.03 mg of electrocatalyst and Au ring as ring electrode. The ring potential was kept at +1.40 V (NHE) during all experiments. The collection efficiency (N = 0.18), was obtained experimentally by using a 5×10^{-3} M $K_3Fe(CN)_6$ solution in 0.1 M K_2SO_4 as electrolyte. All potentials are also referred to NHE.

2.4. Membrane-electrode assembly (MEA) preparation and characterization

Before MEA preparation, $Ru_xM_ySe_z$ (M = Cr, Mo, W) electrocatalysts were ultrasonically mixed with carbon Vulcan at 10, 20 and 40 wt%. These dispersions were used to prepare three series of membrane-electrode assemblies for each electrocatalyst, one series per each dispersion percentage. Each series consisted of 10 membrane-electrode assemblies with different electrocatalyst cathode loading. The catalyst dispersion loading was between 0.2 and 2.0 mg cm^{-2}, with increments of 0.2 mg cm^{-2}.

The anodic catalyst layer was kept constant and consisted of 0.8 mg cm^{-2} at 10 wt% Pt/carbon (E-Teck) loading. The MEA was prepared following a procedure previously described [6]. Briefly it was made by spraying a suspension of ink containing a mixture of 50 μL of Nafion® 5 wt% (Du Pont, 1100 EW) and 1.5 mL of ethanol per each 3.6 mg of Vulcan XC-72 present in the dispersions. The resulting suspension was sprayed onto 112 Nafion® membranes by means of a home fabricated electronic semiautomatic device. The gas diffusion medium at anode and cathode sides were Teflon treated carbon papers (ElectroChem). The membrane and the deposited electrocatalytic materials were hot pressed at 4.4 kg cm^{-2} and 120 °C for 3 min. Fuel cell performance of each MEA was measured at 80 °C and 30 psi pressure for both gases in an ElectroChem Fuel Cell Test System 890B. The fuel cell test station was operated with high purity H_2 and O_2 at 50 cm^3 min^{-1}.

3. Results and discussion

3.1. SEM characterization

Fig. 1(a–c) shows SEM images of as-synthesized $Ru_xM_ySe_z$ powders, with the following average particle size dispersions: $Ru_xCr_ySe_z$ 120.1 ± 29 nm; $Ru_xMo_ySe_z$ 38.0 ± 13 nm and $Ru_xW_ySe_z$ 68.9 ± 38 nm. These average aggregate sizes make mandatory to

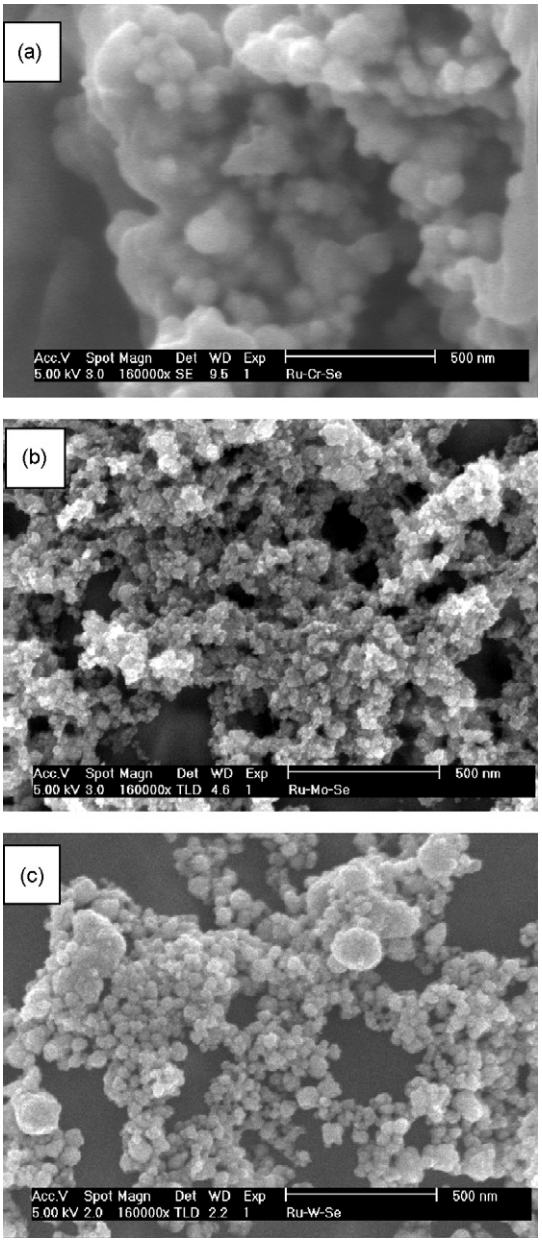

Fig. 1. SEM micrographs of as-synthesized particles of $Ru_xM_ySe_z$ catalyst: (a) $Ru_xCr_ySe_z$, (b) $Ru_xMo_ySe_z$ and (c) $Ru_xW_ySe_z$.

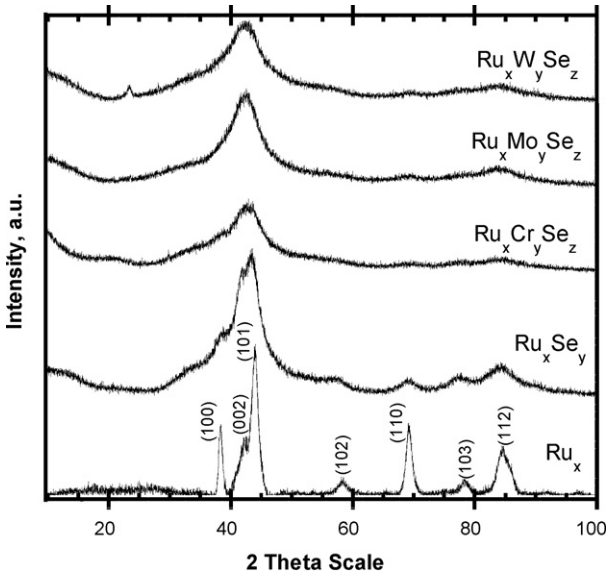

Fig. 2. XRD patterns of nanosized particles of Ru_x, Ru_xSe_y and $Ru_xM_ySe_z$ (M = Cr, Mo, W) as-synthesized in 1,6-hexanediol at 220 °C for 3 h. Assigned peaks correspond to Ru JCPDS card 06-663.

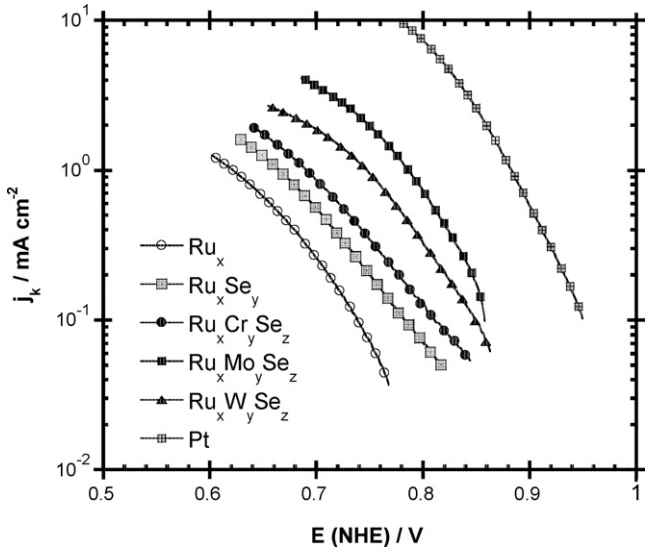

Fig. 3. Mass transfer corrected Tafel plots for the ORR on Ru_x, Ru_xSe_y, $Ru_xM_ySe_z$ (M = Cr, Mo, W) and Pt in O_2-saturated 0.5 M H_2SO_4 at 25 °C.

disperse the material with an appropriate support in order to obtain the maximum catalyst performance in a fuel cell. The estimated average elemental chemical compositions were $Ru_4Cr_1Se_2$, $Ru_6Mo_1Se_3$ and $Ru_{11}W_1Se_6$ as deduced from EDS data from the atomic percent chemical analysis. The content of Ru:Se atomic ratio was almost constant of *ca.* 2:1, whereas the atomic content of the second metal varied according to the following relative order: Cr > Mo > W. It should be kept in mind that these results correspond to an average composition and some of them were twice tested in order to verify reproducibility of these results.

X-ray diffraction patterns of as-synthesized powders of $Ru_xM_ySe_z$ (M = Cr, Mo, W) and Ru_x, Ru_xSe_y, included by comparison are shown in Fig. 2. The Ru_x powder electrocatalyst pattern matches well with the standard patterns of the crystalline hexagonal ruthenium phase (JCPDS Card code 06-663) being this phase the most important structure present in the Ru-based catalysts [11]. For Ru_xSe_y and $Ru_xM_ySe_z$ (M = Cr, Mo, W) powders the XRD diffraction presented more complex patterns with the appearance of several phases, attributed probably to the formation of clusters with low and high nuclearity. The broader peak observed in $Ru_xM_ySe_z$ powders is indicative of a reduction in its crystallite size and of the growing of an amorphous phase. XRD patterns were fitted using Topas software to determine an average crystallite size. The crystalline percentage was determined by using EVA V1.02 software from Bruker. The average crystallite size was about 5 and 4 nm for Ru_x and Ru_xSe_y and a crystalline percentage of Ru_x 52% and Ru_xSe_y 47% [7,11]. The average crystallite sizes deduced for the bimetallic chalcogenides were: $Ru_xCr_ySe_z$ 4.3 ± 0.4 nm; $Ru_xMo_ySe_z$ 2.8 ± 0.2 nm, and $Ru_xW_ySe_z$ 3.3 ± 0.3 nm. After incorporation of the second metal (Cr, Mo or W) in the ruthenium electrocatalyst matrix, the crystalline percentage decreased to $Ru_xCr_ySe_z$ 36%; $Ru_xMo_ySe_z$ 38%, and $Ru_xW_ySe_z$ 40%. These results suggest the presence of Ru-based nanocrystallites involved in an amorphous phase material, as we have been reported recently [6,7].

3.2. Electrochemical characterization by RDE

Fig. 3 shows the mass transfer corrected Tafel plots of Ru_x, Ru_xSe_y, $Ru_xM_ySe_z$ (M = Cr, Mo, W) and Pt obtained from a RDE polarization curves of a O_2-saturated 0.5 M H_2SO_4 solution at 25 °C. The Ru_x presents poor catalytic activity, with high overpotential for the ORR. The incorporation of selenium to ruthenium improves the catalytic activity and reduces the overpotential for the cathodic reaction. Moreover, a marked improvement in the catalytic activity is observed with the incorporation of a second transition metal. An enhanced activity was observed on $Ru_xMo_ySe_z$ with respect to $Ru_xW_ySe_z$ and $Ru_xCr_ySe_z$. This behavior is attributed to the small particle size which has more exposed area per unit mass, in agreement with SEM results. However, its catalytic activity is still low compared to that of platinum considered up to now one of the best electrocatalyst for the oxygen reduction. Table 1 summarizes kinetic results deduced from RDE experiments in sulfuric acid of the bimetallic chalcogenide electrocatalysts. It can be inferred from Tafel slopes values and charge transfer coefficient that in the range of the potential analyzed, the mechanism for the oxygen reduction in acid media is similar. The exchange current density on $Ru_xM_ySe_z$ presents the higher value, followed by $Ru_xW_ySe_z$ and finally $Ru_xCr_ySe_z$. These values are almost one order of magnitude lower to that obtained on Pt under the same experimental conditions.

Temperature dependence of the exchange current density, transfer coefficient and Tafel slope are of fundamental importance in order to determine the apparent activation energy and the enthalpic and entropic contributions to the charge transfer coef-

Table 1
Electrokinetic parameters deduced from Tafel plots in H_2SO_4 at 25 °C [6,8].

Electrocatalyst	b (mV dec^{-1})	α	α_H	α_S (K^{-1})	j_0 (mA cm^{-2})	$\Delta H_r^{0\#}$ (kJ mol^{-1})
Pt	117.8	0.50			9.50×10^{-4}	37 [15]
$Ru_xCr_ySe_z$	116.1	0.51	4.01×10^{-5}	1.84×10^{-3}	3.11×10^{-5}	40.6 ± 0.31
$Ru_xMo_ySe_z$	116.0	0.51	1.66×10^{-5}	1.67×10^{-3}	4.82×10^{-5}	45.6 ± 0.35
$Ru_xW_ySe_z$	119.6	0.49	13.86×10^{-5}	1.32×10^{-3}	3.31×10^{-5}	52.1 ± 0.40

ficient. Specific methodology for the evaluation of the reversible oxygen electrode potential dependence on temperature required for the kinetic parameters determination was already reported [11,12]. The enthalpic (α_H) and the entropic (α_S) contributions to α ($\alpha = \alpha_H + \alpha_S T$) are shown in Table 1. The term α_H is related to the change of electrochemical enthalpy of activation with electrode potential; meanwhile α_S is related to the change of electrochemical entropy of activation with electrode potential. Both of them were calculated from the so-called Conway plots, the reciprocal of the Tafel slope against $1/T$ (not depicted here). The low value of α_H suggests that the entropy transfer coefficient, α_S, the determining factor for the catalytic activity of the electrochemical reaction, indicates that the entropy turnover plays the most important role in the oxygen reaction on the bimetallic chalcogenide electrocatalysts. The dependence of the charge transfer coefficient with temperature could be associated to the cross-interaction of oxygen adsorbed on active sites in the transition adsorbed state, as Conway et al. [13] has been pointed out.

The apparent activation energy, $\Delta E^{\#}$, for the ORR on $Ru_xM_ySe_z$ (M = Cr, Mo, W) electrocatalysts was evaluated in the temperature range of 25–60 °C, from the slope of the Arrhenius equation represented by the relationship: $\Delta E^{\#} = -2.3R(d \log j_0/d(1/T))$. The lowest value of $\Delta E^{\#}$ is for $Ru_xCr_ySe_z$, followed by $Ru_xMo_ySe_z$ and finally $Ru_xW_ySe_z$, which does not correlate with the electrocatalyst activity for the ORR inferred from the Tafel behavior. However, it should be considered that $\Delta E^{\#}$ is a thermodynamic measurement and the activity is strongly influenced by kinetic parameters and the quantity of active sites in electrocatalysts, among others factors.

3.3. Electrochemical characterization by RRDE

The ORR is a multielectron charge transfer reaction which could proceed via several elementary steps. A way to analyze the kinetics of the ORR is by applying the RRDE data to the simple model proposed by Damjanovic et al. [14]. In this model, there are two pathways in which the ORR can occur: a direct four-electron reduction (k_1) and a series pathways involving H_2O_2 as intermediate (k_2, k_3), described as:

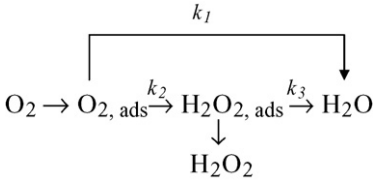

Fig. 4 shows the k_1 and k_2 rate constants ratio calculated from disk and the ring currents and a mass balance over the Damjanovic model. The rate constants k_1 are much larger than k_2 over the potential range explored. This fact confirms that the molecular oxygen reduction on $Ru_xM_ySe_z$ (M = Cr, Mo, W) electrocatalysts are predominantly reduced to water, i.e. $O_2 + 4H^+ + 4e^- \rightarrow 2H_2O$. It can be observed in this figure that the k_1/k_2 ratio of $Ru_xMo_ySe_z$, increases with the overpotential, situation which correlates well with results described below where the favored pathway is the multielectron charge transfer process. Fig. 5 shows the percentage of hydrogen peroxide produced over the bimetallic chalcogenides studied electrocatalysts, being the $Ru_xW_ySe_z$ the one which presents the lowest H_2O_2 formation (<2%). The high H_2O_2 formation is observed on $Ru_xCr_ySe_z$, whereas $Ru_xW_ySe_z$ electrocatalyst presents an intermediate H_2O_2 formation. H_2O_2 formation in these cases does not overpass the 3% and is potential dependent. The subtle differences found between the three electrocatalysts can be explained in terms of the geometric and electronic ambient generated by each transition metal over the Ru–Se matrix and over the active sites. In this subject more research should be carried out in order to explain the observed phenomena.

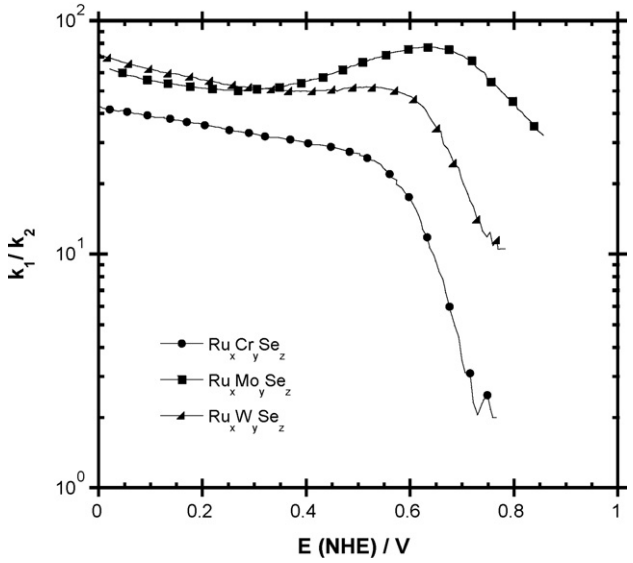

Fig. 4. k_1/k_2 ratio for ORR on $Ru_xM_ySe_z$ (M = Cr, Mo, W) electrocatalysts based on Damjanovic's model at 25 °C.

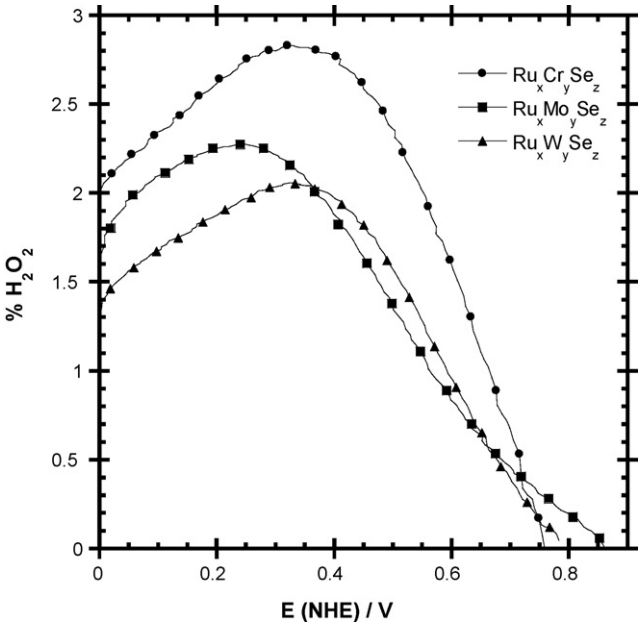

Fig. 5. Percentage of H_2O_2 produced over $Ru_xM_ySe_z$ (M = Cr, Mo, W) electrocatalysts as function of the disk potential.

3.4. PEMFC performance

Each membrane prepared as described previously was tested in order to determine its fuel cell performance. Fig. 6 shows the performance for the best MEAs, one per each electrocatalyst. Naturally, its performance is lower than the Pt performance, but this kind of electrocatalyst is projected to be used in not extensive power-demanding applications or devices. As the best cathode loading in these MEAs is different, it was necessary to normalize the power density obtained on the electrocatalyst content. In this way it was

Table 2
Maximum MEAs performances in power density per unit mass of electrocatalyst.

Electrocatalyst	$w_{maximum}$ (mW cm^{-2})	Dilution, *di*	Cathode loading, *cl* (mg cm^{-2})	Power density per unit mass, W_m (W g^{-1})
Ru_x [7,11]	70	0.33	1.2	176
Ru_xSe_y [7,11]	131	0.33	1.2	328
$Ru_xCr_ySe_z$	227	0.20	1.6	709
$Ru_xMo_ySe_z$	247	0.20	1.0	1235
$Ru_xW_ySe_z$	182	0.40	1.4	325

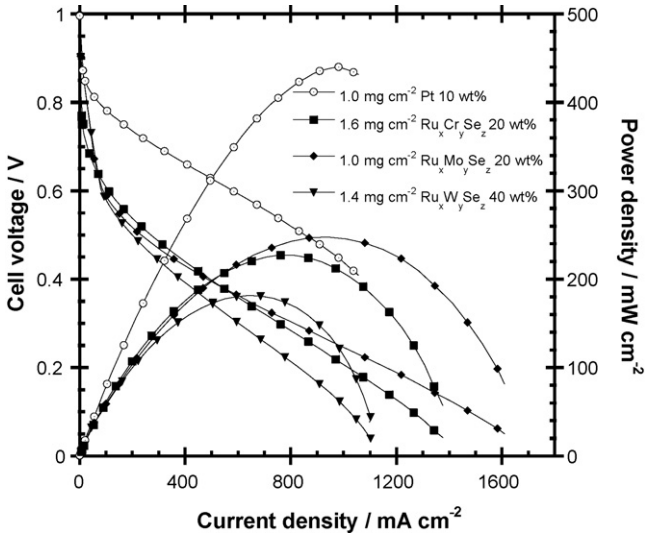

Fig. 6. Performance curves for $Ru_xM_ySe_z$ (M = Cr, Mo, W) electrocatalysts. Best cathode loading performance, operating on H_2/O_2 at 80 °C and 30 psi.

introduced the term W_m, which corresponds to:

$$W_m = \frac{\text{power density}}{\text{catalyst content}} = \frac{w}{cl\,di} \quad (1)$$

where *w* is the maximum power density obtained in each MEA, *cl* is the catalyst loading (0.2–2.0 mg cm^{-2}) and *di* is the catalyst/carbon dispersion ratio (10, 20 or 40 wt%). Table 2 presents in a condensed way the results obtained. In addition, in this table the results of Ru_x and Ru_xSe_y previously reported by our research group were included. Here, it is observed a progressive increase in the performance per mass unit of electrocatalyst (W_m) with the incorporation of selenium and the second transition metal. The performance of the electrocatalyst in the MEAs decreases in activity following the sequence: $Ru_xMo_ySe_z > Ru_xCr_ySe_z > Ru_xW_ySe_z > Ru_xSe_y > Ru_x$. At this point, $Ru_xMo_ySe_z$ electrocatalyst performance agrees well with results of SEM and electrochemical characterization. On the other hand the results of $Ru_xCr_ySe_z$ and $Ru_xW_ySe_z$ electrocatalyst performance are inverted with respect to the electrochemical (half cell) characterization. To explain this phenomenon it should be keep in mind that PEM fuel cell conditions are severe and the materials are exposed to destruction.

4. Conclusions

Ruthenium-based electroelectrocatalysts were synthesized in 1,6-hexanediol and have demonstrated a proper catalytic activity for ORR in acid medium and as a cathodes in a single PEMFC. The SEM and XRD characterization of the synthesized electrocatalysts showed particles with average crystallites around 4 nm in size. The electrocatalyst crystallite size decreases in the following sequence: $Ru_xCr_ySe_z > Ru_xW_ySe_z > Ru_xMo_ySe_z$. The estimated compositions were $Ru_4Cr_1Se_2$, $Ru_6Mo_1Se_3$ and $Ru_{11}W_1Se_6$ and deduced from EDS analysis. The kinetic and fuel cell experiments indicated that the incorporation of a second transition metal to the ruthenium–chalcogenide matrix improves the catalytic activity towards the four-electron reduction of molecular oxygen to water formation. In the charge transfer coefficient the entropy turnover plays an important role on the electrocatalytic process. The value of the apparent activation energy lies in the range of the reported results for other electrocatalysts for ORR in acid electrolyte.

MEA best performance was reached with a cathode catalyst loading of 1.0 mg cm^{-2} of $Ru_xMo_ySe_z$ 20 wt% dispersed in Carbon Vulcan XC-72 and anodic loading of 0.8 mg cm^{-2} Pt 10 wt%/C (E-TEK). This value is the half of the performance obtained with Pt under the same pressure and temperature conditions. The catalytic activity of the ruthenium-based catalyst for the ORR and MEA preparation techniques should be improved to attain at least the same performance as reached with Pt-based electrocatalysts.

Acknowledgements

This work was partially supported by a Grant of National Science and Technology Council of Mexico, CONACYT (Ref. 46094). One of the authors (K.S.A.) would like to thank CONACYT for providing her doctoral fellowship. Also we wish to thank to Institute of Science and Technology of Mexico City, ICTyDF (OCF OSF). The authors thank to Dr. José Chávez - Carlos Flores (IIM-UNAM) and Dr. Gerardo Cabañas (ESFM-IPN) for assistance in XRD and SEM measurements.

References

[1] G. Liu, H. Zhang, J. Phys. Chem. C 112 (2008) 2058–2065.
[2] H. Liu, A. Manthiram, Electrochem. Commun. 10 (2008) 740–744.
[3] C.W. Bezerra, L. Zhang, H. Liu, K. Lee, A. Marques, P. Edmar, H. Wang, J. Power Sources 173 (2007) 891–908.
[4] J.A. Wang, J. Zhang, R.R. Adzic, J. Phys. Chem. A 111 (2007) 12702–12710.
[5] H.A. Gasteiger, S.S. Kocha, B. Sompalli, F.T. Wagner, Appl. Catal. B 56 (2008) 9–35.
[6] K. Suárez-Alcántara, A. Rodríguez-Castellanos, S. Durón-Torres, O. Solorza-Feria, J. Power Sources 171 (2007) 381–387.
[7] R.G. González-Huerta, J.A. Chávez-Carvayar, O. Solorza-Feria, J. Power Sources 153 (2006) 11–17.
[8] K. Suárez-Alcántara, O. Solorza-Feria, Electrochim. Acta 53 (2008) 4981–4989.
[9] J. Junji, D. Cao, A. Wieckoski, K.-C. Chang, A. Menzel, V. Komanicky, H. You, J. Phys. Chem. C 111 (2007) 16889–16894.
[10] J.-W. Lee, B.N. Popov, J. Solid State Electrochem. 11 (2007) 1355–1364.
[11] R.G. González-Huerta, R. González-Cruz, S. Citalán-Cigarroa, C. Montero-Ocampo, J. Chávez-Carvayar, O. Solorza-Feria, J. New Mater. Electrochem. Syst. 8 (2005) 15–23.
[12] A. Parthasarathy, S. Srinivasan, A.J. Appleby, C.R. Martin, J. Electrochem. Soc. 139 (1992) 2530–2537.
[13] B.E. Conway, in: B.E. Conway, R.E. White, J.O.M. Bockris (Eds.), Modern Aspects of Electrochemistry, vol. 16, Plenum Press, 1985, p. 103.
[14] A. Damjanovic, M.A. Genshaw, J.O.M. Bockris, J. Chem. Phys. 45 (1966) 4057–4059.
[15] H. Yano, J. Inukai, H. Uchida, M. Watanabe, P.K. Babu, T. Kobayashi, J.H. Chung, E. Oldfield, A. Wieckowski, Phys. Chem. Chem. Phys. 8 (2006) 4932–4939.